JOURNAL OF MATERIALS SCIENCE 26 (1991) 2293–2299

The study of model polydiacetylene/epoxy composites

Part III *The effect of volume fraction*

I. M. ROBINSON
ICI plc, Wilton Materials Research Centre, PO Box 90, Wilton, Cleveland TS6 8JE, UK

C. GALIOTIS, D. N. BATCHELDER*
*Departments of Materials Science, and *Physics, Queen Mary and Westfield College, Mile End Road, London E1 4NS, UK*

R. J. YOUNG
Department of Polymer Science and Technology, Manchester Materials Science Centre, University of Manchester Institute of Science and Technology, Manchester M60 1QD, UK

Raman spectroscopy and conventional mechanical testing have been employed to study a range of polydiacetylene fibre composite specimens with varying volume fractions cured at either room temperature for a week or at 100 °C for 24 h. The high-temperature cured composites were found to contain thermal stresses sufficient to cause twinning in the polydiacetylene fibres which affected the mechanical response of the bulk composite. A simple modification to discontinuous fibre reinforcement theory which accounts for the effect of thermal stresses in the material has been presented, giving good agreement with the experimental data. Small cracks were found to be produced at the end of the fibres by thermal stresses.

1. Introduction

In the first two papers of this series [1, 2] the axial strain in the fibre and the effect of resin shrinkage in model polydiacetylene (PDA)/epoxy composites were investigated. It was shown clearly that Raman spectroscopy can be successfully employed to measure:

(a) the point-to-point variation of fibre strain in all-polymer composites, as well as the critical transfer length, l_t, required for efficient stress transfer between the matrix and fibre,

(b) the shrinkage stresses induced by the curing cycle of the epoxy resin matrix.

In model PDA composites the strain distribution along the fibre was found to be in qualitative agreement with the shear lag model of Cox [3]. Shrinkage stresses in the epoxy resin induced by high temperatures were found to produce elastic twins in PDA fibres [2, 4]. Composites that were allowed to cure at room temperature were found to be free of residual stresses [2]. The amount of epoxy resin shrinkage produced by high-temperature curing could be determined from the mechanical response of the fibre to an applied strain as measured from frequency shifts in the Raman spectra of the PDA fibre. Variations of the cure temperature produced different degrees of cross-linking in the thermoset epoxy resin. The reduction of volume associated with resin cross-linking, combined with thermal contraction in the case of high-temperature cured specimens produced the shrinkage stresses found in the single-fibre PDA epoxy resin composites. Plotting the amount of resin shrinkage against the differential cure temperature produced an upper bound to the linear thermal expansivity of the epoxy resin matrix [2]. Finally the critical transfer length, l_t, for the efficient stress transfer between the PDA fibre and the epoxy resin matrix was measured as a function of cross-sectional area for model composites cured at room temperature and at 100 °C. The critical transfer length was found to increase linearly with fibre diameter for both types of composite [1, 2] and also to depend upon the applied strain. These results were compared with the Cox model [3] and the predictions of approaches such as finite difference and finite element methods [5, 6].

In the present study, the effect of volume fraction upon the mechanical properties of full composites was examined in detail for epoxy matrices cured at room temperature or at 100 °C for 24 h. Conventional mechanical testing was employed to examine the deformation of the bulk material and of the embedded fibres within the composite. The resultant fracture surfaces were examined by scanning electron microscopy and useful conclusions were drawn for the strength of the fibre/matrix adhesion.

2. Experimental procedure

2.1. Materials

2.1.1. Polydiacetylene fibres

The substituted diacetylene monomer 1-6-di-(*N*-carbazolyl)-2,4-hexadiyne (DCHD) was synthesized

0022–2461/91 $03.00 + .12

and crystallized in the form of a fibre as described previously [1, 7]. The fibres were polymerized by exposure to 30–40 Mrad of ^{60}Co γ radiation. The polymer chains form parallel to the long axis of the fibre as a result of the topochemical polymerization reaction yielding single-crystal polymer fibres [8]. The fibres have a Young's modulus of 45 $\pm$ 1 GPa in the axial direction [7, 8]. The fracture strength of selected defect-free crystals are diameter-dependent ranging from 0.5–1.5 GPa [7, 8]. Fracture strength values for PDA fibres selected at random were found to be two to three times smaller than the data obtained from selected defect-free crystals [8]. This is thought to be due to the presence of crystal growth imperfections and handling defects in the fibres [8]. The fibre cross-sections were approximately hexagonal. The fibre diameters were calculated using a cylindrical cross-section with an equivalent area to the cross-section of the hexagonal PDA–DCHD fibres. Fig. 1 shows the histogram of fibre diameters measured from a sample of 250 fibres obtained at random; Fig. 2 shows the matching data for the fibre lengths. Using the data presented in Figs 1 and 2, typical fibre diameters and lengths have been calculated. These are: diameter, $d = 59 \pm 28$ μm and length, $l = 6.3 \pm 2.4$ mm. This yields a typical fibre aspect ratio (fibre length to diameter) of approximately 100:1.

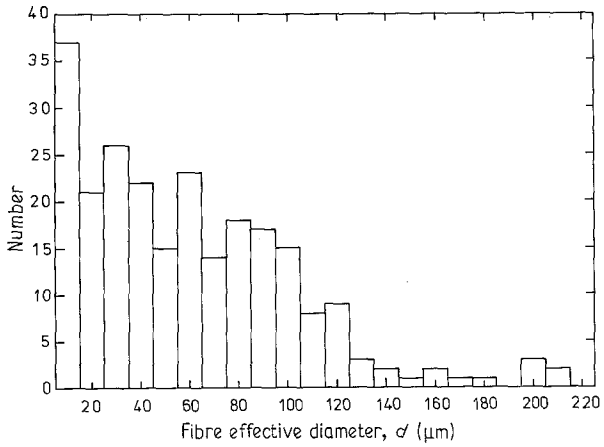

Figure 1 Histogram of PDA–DCHD fibre diameters for 250 fibres selected at random.

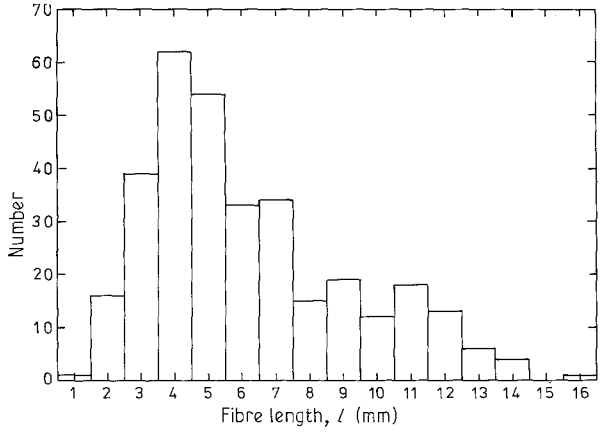

Figure 2 Histogram of PDA–DCHD fibre lengths for 250 fibres selected at random.

2.1.2. Epoxy resin matrix

All the composites used in this study were prepared with Ciba Geigy XD 927 two-part solvent-free epoxy resin using 36% wt/wt hardener to resin. Two distinct methods were used to cure the epoxy resin. In all cases the epoxy resin was mixed to the correct proportions, placed in a simple mould and after the addition of PDA–DCHD fibres (with random lengths, diameters) were allowed to set at room temperature for 24 h. The partially cured composite specimens were then fully cured using either method (a) or (b) as follows.

(a) The composite specimens were placed in an oven at 100 °C for a further 24 h and were subsequently cooled back to room temperature.

(b) The composite specimens continued to set at room temperature for a further week.

2.2. Composite preparation

Two types of specimen geometry were prepared from the PDA–DCHD epoxy composites cured by either method (a) or (b). Specimens tested by conventional mechanical means were prepared in the following manner. Fibres were aligned approximately parallel to each other in a steel mould with overall dimensions of 38 mm × 6 mm × 5 mm. The epoxy resin was introduced into the mould, covering the fibres. More fibres were added, approximately aligned and were covered with the addition of more resin. In this manner a layered structure was built up until deemed to be sufficiently thick. Excess resin was removed by the application of pressure using a steel bar fitted to the top of the mould, producing composite specimens in the region of 1–1.5 mm thick, and a variety of fibre volume fractions. The samples were then cured using either method (a) or (b) as described in Section 2.1.2. After curing, aluminium tabs with dimensions of 10 mm × 5 mm × 1 mm were glued using the XD 927 epoxy resin to the ends of the composite bar while thin-film strain gauges of gauge factor 2.1 were placed on the surface of the composite using a cyanoacrylate adhesive.

Composites tested using Raman spectroscopy were prepared in a similar manner to that used by Galiotis *et al.* [1]. A PTFE dog-bone shaped mould was filled with the mixed epoxy resin and PDA–DCHD fibres were introduced into the resin and aligned using fine steel needles. The specimens were allowed to set and were cured using either method (a) or (b). After polishing to give good optical transmission, thin-film resistance strain gauges of gauge factor 2.1 were attached to the surface of the specimens using a cyanoacrylate adhesive. The finished composites were then drilled in the tab regions, ready for mounting in the loading device.

2.3. Mechanical tests

The mechanical tests were performed on an Instron Universal screw-driven testing machine, using a load cell with a maximum capacity of 5 kN. The composite bars shown in Fig. 3 were mounted in the jaws of standard friction grips. All the tests were performed at

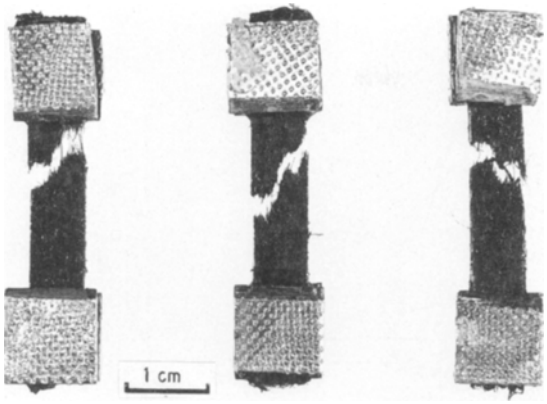

Figure 3 Typical PDA–DCHD fibre composites tested in tension until failure occurred.

$22 \pm 2\,^{\circ}C$, using a crosshead displacement rate of $5\,mm\,min^{-1}$. The fracture stress of each bar was determined from the maximum load (measured from the load/displacement trace) divided by the original bar cross-sectional area. The strain was measured using resistance strain gauges with an accuracy of $\pm 0.01\%$. The modulus for each sample was determined from the initial slope of the stress–strain trace.

2.4. Raman spectroscopy

The composite bars were mounted between the jaws of a small tensile loading device which was mounted on a micrometer slide. This enabled the full length of the composite bar to be traversed through the incident laser beam. The resonance Raman spectra were excited using the 632.8 nm line from a He–Ne laser operating at 10 mW intensity. The scattered light was collected with the 180° backscattering geometry using the SPEX 1401 double monochromator and photon counting system. A line focus of approximately 5 mm length was produced on the surface of the PDA–DCHD composite bars by a cylindrical lens. This ensured that the Raman spectra were produced by scattering from a large number of PDA–DCHD fibres embedded in the epoxy resin bar. The triple bond carbon–carbon stretching mode, situated at $2085\,cm^{-1}$, was used to measure the average fibre strain [1, 4, 9]. The band centre could be determined to within $\pm 2\,cm^{-1}$; however, Raman frequency shifts could be measured within an accuracy of $\pm 0.2\,cm^{-1}$. Because the $2085\,cm^{-1}$ Raman band for PDA–DCHD shifts to lower frequency by $-19.7\,cm^{-1}/\%$ strain, the fibre average strain could be measured to within $\pm 0.01\%$.

2.5. SEM studies

The fracture surfaces of the composite bars were examined in a Joel 50 A scanning electron microscope operating at an accelerating voltage of 10–15 keV. The surfaces were made conductive by sputter coating with a thin layer of gold and electrically grounded with silver paint. The magnification was calibrated using a fine mesh of known dimensions.

2.6. Volume fraction determination

Values for the fibre volume fraction for each of the composite specimens were determined from the bars after fracture had occurred. The composite bars were sectioned in a number of places and the surfaces were polished and examined using reflectance optical microscopy.

3. Results and discussion

3.1. Curing-induced shrinkage stresses

A transmission optical micrograph for PDA–DCHD composite sample with $V_f = 12\%$ is shown in Fig. 4. The range of fibre orientations within the composite can be seen in Fig. 5; approximately 70% of the fibres were found to be axially oriented within $\pm 30°$ of the direction of applied load. Close examination of Fig. 4

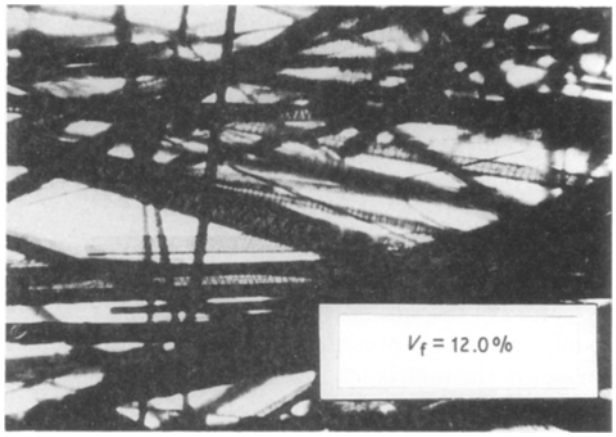

Figure 4 Transmission optical micrograph (× 40) for a PDA–DCHD composite specimen with $V_f = 12\%$, cured at 100 °C for 24 h.

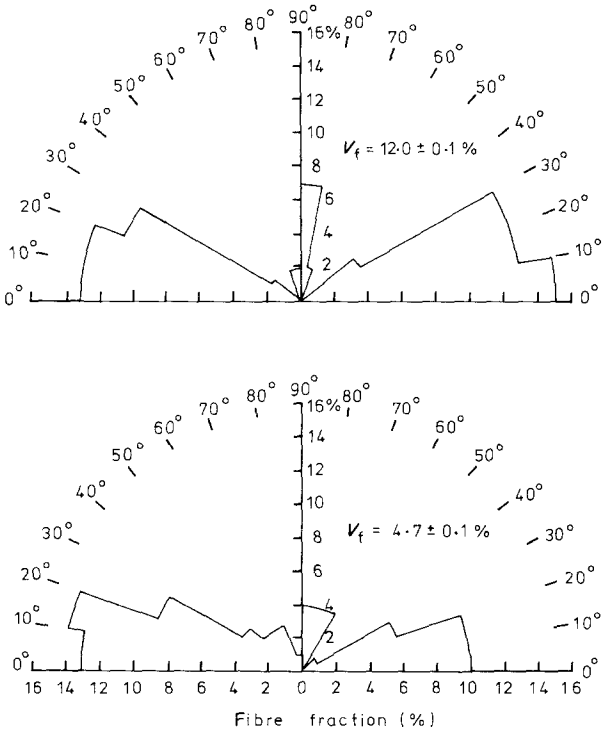

Figure 5 Normalized histogram of the fibre orientation distribution for two PDA–DCHD composite specimens with $V_f = 5\%$ and 12%.

revealed that the bulk of the PDA–DCHD fibres had undergone twinning as a result of the composite being cured at high temperature via method (a) (see Section 2.1.2). The twins can be seen in Fig. 4 as the regular zigzag pattern crossing the fibres. Such phenomena have been found in single-fibre PDA–DCHD/epoxy composites [2, 4, 10, 11]. The twinning process relaxes compressive stresses induced in the fibre by the high-temperature curing of the epoxy resin.

The thermally induced twinning dominates the mechanical response of the PDA–DCHD fibres for low-volume fraction composites at small strains, as can be seen in Fig. 6. The mean fibre strain, determined from the shift in the 2085 cm^{-1} Raman band, is plotted as a function of the applied matrix strain, as determined by the attached resistive strain gauge, for three composite samples with $V_f = 5\%$, 12% and 50%, respectively. The two straight lines in Fig. 6 are those expected for the limiting case where: (i) the strain in the fibre and matrix are equal, Voigt-type (V) behaviour; (ii) the stress in the fibre and matrix are equal, Reuss-type (R) behaviour. For the V_f values of 5% and 12% the Reuss line is followed at low strains. Twinning of the fibres has occurred during curing so the effective fibre length is very short, approximately the distance between twin bands, so Reuss-type behaviour is expected until the strain is sufficiently high to have removed elastically all the stress-induced twins. By contrast, the specimen with V_f equal to 50% has insufficient resin present to produce the residual stresses in the matrix (caused by thermal contraction) necessary to induce twinning of the PDA–DCHD fibres. The effective fibre length is now its actual length, so Voigt-type behaviour is expected.

The strain required to take the fibres into Voigt type behaviour gives a measure of the thermally induced shrinkage strains which initiate fibre twinning. This can be estimated from the data by fitting a line to the higher strain data and extrapolating this line back to the applied strain axis. The intercept with this axis is defined as $\varepsilon_{shrinkage}$, the applied strain required to overcome the thermally induced shrinkage stresses and subsequent fibre twinning [2, 4]. Fig. 7 shows the

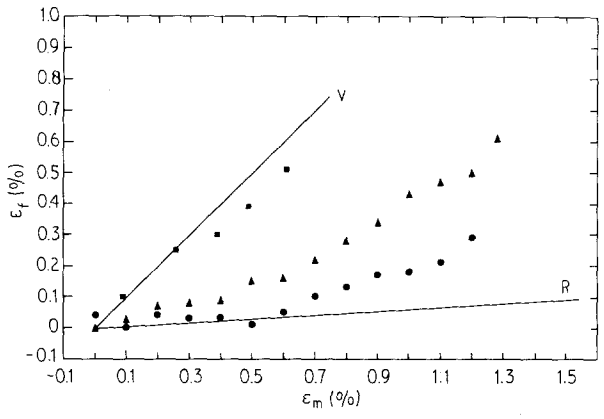

Figure 6 Average fibre strain versus applied composite strain for three different volume fraction specimens. V_f = (●) 4.7%, (▲) 12.0%, (■) 49.9%.

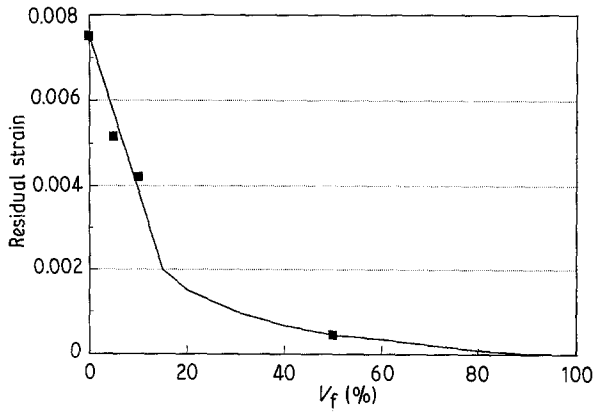

Figure 7 Resin shrinkage strain, fibre against volume fraction for a series of different volume fraction PDA–DCHD composite specimens. The curve is an empirical fit to the data.

dependence of shrinkage upon the volume fraction. The experimental points at $V_f = 5\%$, 12% and 50% are taken from Fig. 6 while that for $V_f = 0$ was taken from Fig. 5 of [1] for a single-fibre PDA–DCHD composite. The solid line in Fig. 7 represents an attempt to predict the shrinkage behaviour of the composites using a simple two-stage model which has two basic assumptions. Firstly the shrinkage is assumed to be entirely due to the thermal contraction of the composites between 100 °C curing temperature and room temperature. This neglects any possible effects of matrix contraction due to the curing process itself; so far none have been detected in measurements made at the curing temperature. Secondly, it is assumed that the PDA–DCHD fibres relieve the stresses of thermal contraction by twinning when the resultant strain of the composite exceeds 0.2% [4]. Below this value of strain the fibres are assumed to offer no further resistance to the thermal contraction of the matrix.

Parallel to the fibre direction, the thermal expansion coefficient of a fully aligned composite has been shown to be [19]

$$\alpha_{11} = \frac{E_f\alpha_f V_f + E_m\alpha_m(1 - V_f)}{E_f V_f + E_m(1 - V_f)} \quad (1)$$

where E_f and E_m are the elastic moduli and α_f and α_m are the thermal expansivities of the fibre and matrix, respectively. Application of Equation 1 to the PDA–DCHD/epoxy composite system leads to the conclusion that, on curing to 20 °C from 100 °C, the critical V_f for twin formation is approximately 15%. These calculations produced the solid line in Fig. 7 for values of $V_f > 15\%$. For lower values of V_f, twinning will occur at a temperature greater than room temperature. Equation 1 has been used to predict these temperatures, below which the fibres are assumed to offer no effective resistance to thermal contraction. The solid line in Fig. 7 for values of $V_f < 15\%$ has been calculated by assuming that the thermal expansivity of the composite is just $\alpha_m(1 - V_f)$. Fitting the data to the point at $V_f = 0$ gave a value of $\alpha_m = 9.4 \times 10^{-5}\,°C^{-1}$.

The agreement between this very simple model for thermal shrinkage and the limited experimental data

which are shown in Fig. 7 suggests that the assumptions which have been made are reasonable. One factor which certainly limits the degree of accuracy with which predictions can be made is the dependence of the critical strain for twin formation upon fibre orientation. Under tensile stress, however, we have drawn the conclusion from Fig. 7 that the shrinkage strains in the PDA–DCHD/epoxy system studied here have a negligible effect on the elastic modulus and strength of the composites for $V_f > 15\%$.

3.2. Mechanical tests

3.2.1. Modulus versus fibre volume fraction

A typical stress–strain curve for a composite specimen with $V_f = 55\%$ is given in Fig. 8. The data showed a linear response up to failure at 118 MPa. In Fig. 9 the modulus for a series of composite specimens at different volume fractions has been plotted. The data marked by solid circles correspond to composites cured at high temperature using method (a) whereas the data plotted by open circles correspond to composites cured at room temperature under method (b) (see Section 2.1.2). It can be seen that neither the Voigt model (V) nor the Reuss model (R) can adequately explain the data. Instead an empirical model marked by the line (M) has been employed.

For a uniaxially aligned continuous fibre composite the "rule of mixtures" gives an expression for the tensile modulus [13] in the direction of fibre reinforcement, E_{11}

$$E_{11} = E_f V_f + E_m(1 - V_f) \quad (2)$$

The PDA–DCHD/epoxy composites are composed of fibres with a distribution of lengths, diameters, strengths and orientations within the composite. Consequently, Equation 2 must be modified to take account of some of these variables

$$E_{11} = f(l_t)f(\theta)E_f V_f + E_m(1 - V_f) \quad (3)$$

The term $f(l_t)$ gives a measure of the critical transfer length for the fibre and denotes the amount of fibre giving efficient reinforcement [3]. At first approximation

$$f(l_t) = 1 - \frac{l_t}{2 \cdot l^{av}} \quad (4)$$

where l^{av} is the average value obtained from the distribution of fibre lengths. The expression has been calculated for the typical fibre aspect ratio of 100:1 found from Figs 1 and 2 and the critical transfer length has been calculated from the data presented in Fig. 8 of [1].

Realistically the critical transfer length term should be represented by a summation term over all fibre lengths and diameters. It should also be noted that the critical transfer length for a composite is dependent upon the fibre/matrix modulus ratio and adhesion between the two phases; $f(l_t)$ is also dependent upon the temperature, applied load and time under load as well as a range of geometrical factors [1, 2, 6, 13]. The term $f(\theta)$ represents the orientation distribution function for the fibres and can be expressed to a first approximation by an integral of the components of applied strain in the fibres acting along the direction of the load

$$f(\theta) = \int \cos^2(\theta)\, d\theta \quad (5)$$

The term $f(\theta)$ has been calculated from a summation of the components of stress with the orientation distribution given in Fig. 3. Note that this expression only applies to composites containing untwinned fibres; that is, in this case, for $V_f > 15\%$.

After calculation the critical transfer length $f(l_t)$ was found to be 0.78 and the orientation function $f(\theta)$ to be 0.92. This is sufficient information to plot the line given by Equation 3, corresponding to the composites cured at room temperature and is shown by the line marked (M) in Fig. 9. The experimental data points for the composites cured at room temperature are shown by the open circles and are clustered about the model line. As predicted by the discussion in Section 3.1, there is no consistent difference in the behaviour of composites cured at room temperature and those at 100 °C, as there were only two samples with $V_f < 15\%$. Overall the agreement between the model described above is good given the assumptions made.

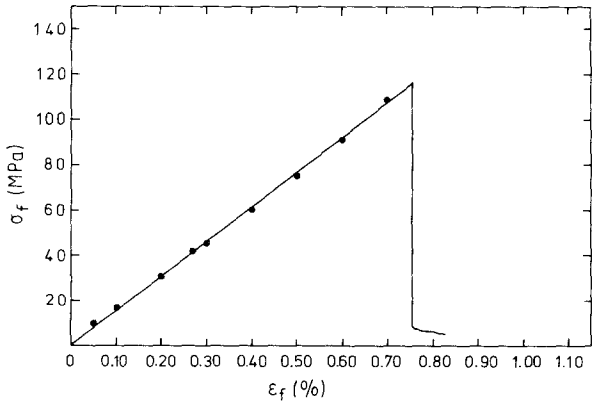

Figure 8 Typical stress–strain curve for a PDA-DCHD composite specimen with $V_f = 55\%$.

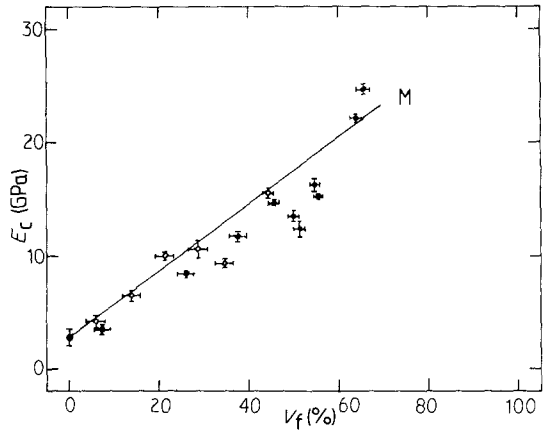

Figure 9 Modulus (measured from the initial slope of the stress–strain data) against volume fraction for a range of composite specimens, cured at room temperature (open circles) and at 100 °C (filled circles).

3.2.2. Fracture strength versus fibre volume fraction

The process of fracture in discontinuous fibre composites is complex. The stress–strain curve, as well as the fracture strains for both the XD927 epoxy matrix, ε_m^* and a PDA–DCHD, ε_f^* are plotted together in Fig. 10. In this instance $\varepsilon_m^* > \varepsilon_f^*$. Consequently, for low volume fraction composites the fracture process is essentially governed by stress concentrations in the matrix due to the discontinuous fibres. In the case of single-fibre PDA–DCHD composites cured at high temperature, mushroom-shaped cracks about the fibre ends have been detected [6]. Fig. 11 shows such a crack, thought to be due to stresses formed by resin expansion on curing at elevated temperatures. Such cracks will drastically effect the fracture strength of low volume fraction composites and their presence at higher values of V_f would be detrimental as well.

The fracture strengths for a series of composite samples cured by both methods (a) and (b) are plotted in Fig. 12. The data for composites cured at room temperature are shown with open circles; the solid data points represent the data for composites cured at higher temperature. At low volume fractions ($V_f < 15\%$) the presence of stress concentrations reduced the fracture strength of the composite compared to the resin. For $V_f > 15\%$ a different behaviour occurred. An expression for the fracture strength in the discontinuous fibre composites can be given by

$$\sigma_{11}^* = A\sigma_f^* + B\sigma_m^*(1 - V_f) \qquad (6)$$

where σ_f^*, σ_m^* represent the fracture strengths of the fibre and matrix, respectively, and constants A and B are terms that account for the variability in fibre fracture strength and the effect of stress concentrations in the matrix, respectively. A can be calculated using Rosen's expression for the mean fracture strength of a bundle of fibres [15]; B can be accounted for if the number and types of flaws in the composites are known.

The data shown in Fig. 11 of [8] have shown that perfect PDA–DCHD fibres have a fracture strength dependent upon fibre diameter. Imperfect fibres show a similar dependency upon diameter although with a lower mean fracture strength by about a factor of two to three. Given the typical values for PDA–DCHD fibre diameters shown in Fig. 1 ($d = 59 \pm 28$ μm) the mean fracture strength for perfect fibres can be estimated from the data in [8] to be 690 ± 140 MPa. Placing this value in Equation 6 produces a curve similar to that for the experimental data in Fig. 12 with the exception that the values are about three times larger than those observed. As mentioned, the mean fracture strength for imperfect fibres is somewhat lower; the manner in which the composites are prepared will also reduce the mean fibre strength and produce flaws in the bulk of the material which could account for the discrepancy between measure and expected composite fracture strength. The composites cured at room temperature display higher fracture strengths than those for the higher temperature cured samples. This is due largely to the absence of the cracks shown in Fig. 11 produced by the thermal stresses. For $V_f > 55\%$ there is a large fall in the fracture strength for the high-temperature cured composites. This is thought to be due to "bunching" of

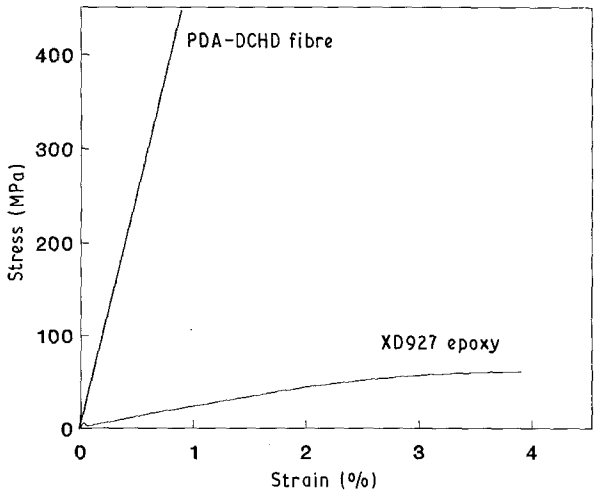

Figure 10 Stress–strain curves of a typical PDA–DCHD fibre and for a tensile bar of XD927 epoxy resin. The initial modulus of the resin has been measured from the slope of the dashed line.

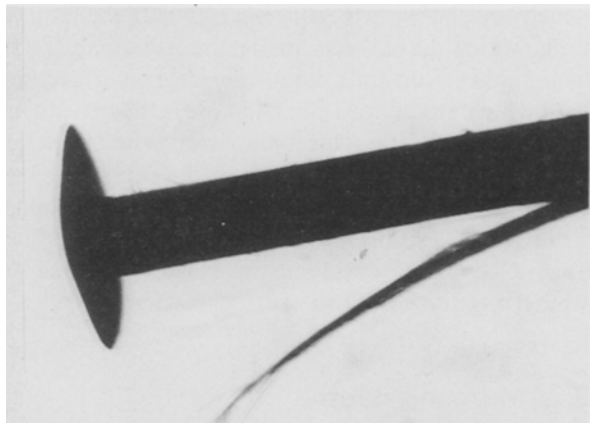

Figure 11 Thermal induced mushroom shaped crack found at the end of a single PDA–DCHD fibre composite cured at 100 °C, × 160.

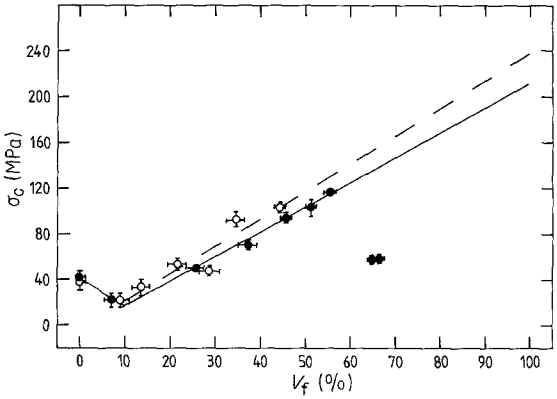

Figure 12 Fracture strength against volume fraction for a range of PDA–DCHD composite specimens cured at room temperature (open circles) and at 100 °C (filled circles).

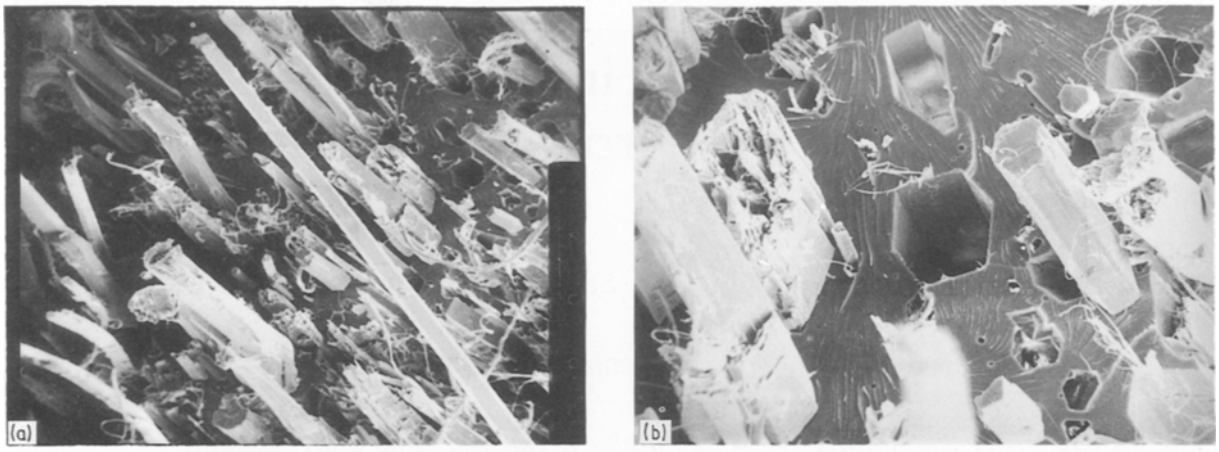

Figure 13 (a) Typical fracture surfaces for a PDA–DCHD composite specimen displaying fibre pull-out. (b) Higher magnification image of fibre pull-out from PDA–DCHD composite specimen.

fibres of different diameters brought about by the high moulding pressures required to obtain $V_f > 55\%$.

A typical fracture surface for a composite specimen can be seen in Fig. 13. The hexagonal cross-sectional shape of the PDA–DCHD fibres have been resolved together with the fibre impressions left in the epoxy matrix due to fibre debonding and pull-out. The presence of fibre pull-out indicates that the fibre/matrix bonding across the interface is less than perfect [12, 13, 14].

4. Conclusions

PDA–DCHD fibre composites are ideal materials for examining the behaviour of discontinuous fibre composites. The mechanical response of single PDA–DCHD fibre composites is well understood and the importance of resin shrinkage on the physical behaviour has been demonstrated for low volume fraction composites as well. A simple correction to standard composite theory has been developed to account for the increase of the composite modulus with fibre volume fraction which gives good agreement with the experimental data. Small cracks have been found in samples cured at high temperature that can affect the stress distribution within the composite.

References

1. C. GALIOTIS, R. J. YOUNG, P. H. J. YEUNG and D. N. BATCHELDER, *J. Mater. Sci.* **19** (1984) 3640.
2. I. M. ROBINSON, R. J. YOUNG, C. GALIOTIS and D. N. BATCHELDER, *ibid.* **22** (1984) 3642.
3. H. L. COX, *Brit. J. Appl. Phys.* **3** (1952) 72.
4. I. M. ROBINSON, P. H. J. YEUNG, C. GALIOTIS, R. J. YOUNG and D. N. BATCHELDER, *J. Mater. Sci.* **21** (1986) 3440.
5. Y. TERMONIA, *ibid.* **22** (1987) 1733.
6. I. M. ROBINSON, PhD thesis, University of London (1987).
7. C. GALIOTIS, PhD thesis, University of London (1984).
8. C. GALIOTIS, R. T. READ, P. H. J. YEUNG, R. J. YOUNG, I. F. CHALMERS and D. BLOOR, *J. Polym. Sci. Polym. Phys. Edn* **22** (1984) 1569.
9. D. N. BATCHELDER and D. BLOOR, in "Advances in Infrared and Raman Spectroscopy", Vol. 11, edited by R. J. H. Clark and R. E. Hester (Wiley, Chichester, 1983) p. 133.
10. R. J. YOUNG, D. BLOOR, D. N. BATCHELDER and C. L. HUBBLE, *J. Mater. Sci.* **13** (1978) 62.
11. P. H. J. YEUNG, PhD thesis, University of London (1984).
12. C. C. CHAMIS, in "Composite Materials", Vol. 6, edited by E. D. Plueddemann (Academic Press, New York, 1974) p. 32.
13. D. HULL, "An introduction to composite materials" Cambridge Solid State Science Series (Cambridge University Press, 1981) p. 83.
14. A. KELLY, *Proc. R. Soc. Lond.* **A319** (1970) 95.
15. B. ROSEN, *ibid.* **A319** (1970) 79.

Received 27 July
and accepted 9 August 1990